HHS Public Access

Author manuscript

J Pathol. Author manuscript; available in PMC 2017 March 01.

Published in final edited form as:

J Pathol. 2016 March ; 238(4): 571–583. doi:10.1002/path.4680.

Low-grade inflammatory polarization of monocytes impairs wound healing

Ruoxi Yuan[*,1], **Shuo Geng**[*,1], **Keqiang Chen**[*,1], **Na Diao**[1], **Hong Wei Chu**[2], and **Liwu Li**[1,#]

[1]Department of Biological Sciences, Virginia Tech, Blacksburg, VA 24061-0910

[2]Department of Medicine, National Jewish Health, Denver, CO

Abstract

Impaired wound healing often accompanies low-grade inflammatory conditions during which circulating levels of subclinical super-low dose endotoxin may persist. Low-grade inflammatory monocyte polarization may occur during chronic inflammation and deter effective wound repair. However, little is understood about the potential mechanisms of monocyte polarization by sustained insult of subclinical super-low dose endotoxin. We observed that super-low dose endotoxin preferentially programs a low-grade inflammatory monocyte state *in vitro* and *in vivo*, as represented by the elevated population of $CD11b^{+}Ly6C^{high}$ monocytes and sustained expression of CCR5. Mechanistically, super-low dose endotoxin caused cellular stress, altered lysosome function and increased the transcription factor IRF5. TUDCA, a potent inhibitor of cellular stress, effectively blocked the monocyte polarization, and improved wound healing in mice injected with super-low dose endotoxin. Our data reveal the polarization of low-grade inflammatory monocytes by sustained endotoxin challenge, its underlying mechanisms, and a potential intervention strategy.

Keywords

innate immunity; low-grade inflammation; wound healing; monocytes; IRF5; cellular stress

Introduction

Monocytes play key roles during the progression and resolution of various inflammatory processes. Past studies reveal the dynamic existence of distinct subtypes of innate monocytes in mice and humans. Murine monocytes are represented by $CD11b^{+}$ $Ly6C^{high}$ inflammatory monocytes and $CD11b^{+}Ly6C^{-}$ anti-inflammatory monocytes [1]. In humans,

[#]Correspondence to: Liwu Li, PhD, Dept. of Biological Sciences, Virginia Tech, Life Science 1 Bldg., 970 Washington St., Blacksburg, VA 24061. Tel.: 1-540-2311433; Fax: 1-540-2314043; lwli@vt.edu.

[*]Equal contribution

Conflict of Interest Statement:
The authors claim no competing conflict of interest.

Author contributions:
L.L.: study design, data analysis and manuscript preparation; R.Y.: study design, data collection, data analysis, and manuscript preparation; S.G.: study design, data collection, data analysis, and manuscript preparation; K.C.: study design, data collection, data analysis, and manuscript preparation; N.D.: data collection, data analysis, and manuscript preparation; H.C.: manuscript preparation.

there are three circulating subsets that include the classical $CD14^{++}CD16^{-}$, the non-classical $CD14^{+}CD16^{++}$, and the intermediate $CD14^{+}CD16^{+}$ monocytes [2]. Current literature suggests that the intermediate human monocytes share most similarities with the murine $CD11b^{+}Ly6C^{high}$ inflammatory monocytes in their expression profiles of inflammatory mediators, and may be closely correlated with the severity of chronic inflammatory diseases [2–4]. However, molecular mechanisms leading to the expansion of the inflammatory monocytes are not clearly understood.

In the context of the wound repair process in murine models, the initial influx of inflammatory $Ly6C^{high}$ monocytes into the cutaneous wound bed may be important for the early phase of vascular sprouting [5]. Subsequent transition into the anti-inflammatory $Ly6C^{-}$ monocytes would enable proper wound closure and tissue regeneration during the resolving phase of wound repair [5,6]. The switch from an initial inflammatory state to a subsequent compensatory anti-inflammatory state is critical for ordered wound repair. Persistence of inflammatory monocytes in the wound bed may be an important factor underlying poorly healing wounds, as often seen in diabetic patients [7].

Subclinical super-low dose endotoxin lipopolysaccharide (LPS) in the circulation has been increasingly recognized as a health concern [8]. Chronic infection, obesity, aging, chronic smoking and drinking are common risk factors that contribute to mucosal leakage and elevated plasma levels of endotoxin [9,10]. There remains an intriguing correlation that super-low dose endotoxemia may underlie diabetes and obesity-associated complications such as impaired wound healing [11–16].

Recent mechanistic studies may support the correlation between super-low dose endotoxemia and low-grade non-resolving inflammation [8]. Higher doses of LPS cause robust yet transient induction of inflammatory mediators, followed by “endotoxin tolerance”, a state of compensatory resolution to restore homeostasis through various processes such as autophagy completion [17–19]. In sharp contrast, super-low levels of LPS (~1–100 pg ml^{-1}) fail to induce homeostatic tolerance [20,21]. Our *in vitro* studies suggest that the disruption of compensatory feedback mechanisms such as the completion of autophagy and the resolution of cellular stress may be a culprit [20,22].

One key limitation to the existing studies of the dynamic monocyte priming and tolerance paradigm is the short time course being examined. Most studies involve only one LPS treatment to induce priming or tolerance within a 24-hour time period. To better examine the sustained polarization of monocytes, we aim to test the hypothesis that sustained challenges with super-low dose LPS may polarize monocytes into a low-grade inflammatory state, not conducive for effective wound healing.

To test this hypothesis, we examined the behavior of monocytes challenged with sustained super-low dose LPS *in vitro* and *in vivo*, as well as that of human monocytes. Using a cutaneous wound healing animal model, we examined the pathological consequence of subclinical dose LPS *in vivo*. We also test the therapeutic potential of tauroursodeoxycholic acid (TUDCA), a potent inhibitor of cellular stress, in restoring lysosome function, monocyte homeostasis and effective wound repair affected by subclinical dose LPS.

Materials and Methods

Animals

C57BL/6 mice were maintained and bred under standard pathogen-free conditions. 8–12-week-old male animals were used. Experiments were approved, prior to the study, by the Institutional Animal Care and Use Committee (IACUC) of Virginia Tech.

Reagents

LPS (*Escherichia coli* 0111:B4) was purchased from Sigma (St. Louis, MO). TUDCA was purchased from Prodotti Chimici E Alimentari S.p.A (Basaluzzo, Italy). Murine macrophage colony-stimulating factor (M-CSF), CCL3 and CCL5 were obtained from PeproTech (Rocky Hill, NJ). Anti-mouse monocyte/macrophage marker (MOMA-2) antibody and anti-phospho-JNK were purchased from Santa Cruz (Dallas, TX); anti-mouse CD 16/32 antibody, anti-mouse Ly-6G (Gr-1) antibody, biotin-anti-mouse IgG, biotin-anti-rat IgG and streptavidin-PE, streptavidin-FITC were from eBioscience (San Diego, CA). PE-rat anti-mouse CD31 antibody and biotin-goat anti-rabbit Ig antibody were from BD Pharmingen (San Jose, CA). PE-anti-mouse TGF-β antibody and streptavidin-HRP were from Biolegend (San Diego, CA). Anti-neutrophil antibody (7/4) was from Abcam (Cambridge, MA). Dab substrate kit for peroxidase was from Vector Laboratories (Burlingame, CA). Anti-SAPK/JNK antibody was obtained from Cell Signaling Technology.

Wounding procedure and LPS treatment protocol

The wound repair model was as previously described [23–25]. Briefly, anesthetized mice were partially shaved at the back, and sterilized with betadine solution followed by 70% ethanol. Four full-thickness punch biopsies (Acu.Punch, 6 mm, Acuderm, FL) were created. The biopsy sites were covered with a form-fitting bandage. Mice were injected IP with either PBS or LPS (5 ng/kg body weight) once every three days for 10 days (total three times) before biopsy and once every three days after biopsy (Fig. 1a). Wounds were monitored daily and photographed using a Nikon 9000D digital camera (Nikon, Japan). Changes in wound contraction over time were calculated using the NIH ImageJ software. For histologic analysis, wounds were excised at different times after injury, and the tissue was either fixed overnight in 10 % formaldehyde or embedded in optimal cutting temperature compound (OCT), (Tissue-Tek, Zoeterwoude, NL).

Histopathology and immunohistochemistry

Skin tissues embedded in OCT were sectioned (4 μm) and stained with H&E. Collagen staining was performed with elastic stain kit (Sigma, St. Louis, MO) in which elastin stains black and van Gieson's solution stains collagen red and other components yellow. 10-μm cryosections were immunostained for the macrophage marker MOMA-2 and for the neutrophil marker Ly-6G. The secondary antibody was biotinylated rabbit anti-rat IgG antibody. The slides were developed using streptavidin–horseradish peroxidase, followed by diaminobenzidine, after which they were counterstained with Mayer's hematoxylin. For immunofluorescence, frozen sections (10 μm) were stained with antibodies as indicated on figure legends.

Cytokine Assay from Plasma

Whole blood samples were collected from naïve, PBS-treated, LPS-treated mice, and plasma samples were obtained by centrifugation. Serum cytokine levels were examined by ELISA according to the manufacturer's instructions (eBioscience, San Diego, CA).

Protein extraction and analyses

Cells were washed with cold PBS after specified treatments and harvested in SDS lysis buffer containing protease and phosphatase inhibitors as previously described [26]. Protein concentration was assessed by Bradford assay. Following SDS-PAGE, protein bands were transferred to an immunoblot PVDF membrane (Bio-Rad) and subjected to immunoblot analysis with the indicated antibodies.

Real-time RT-PCR

Total RNA was extracted using TRIzol (Thermo Fisher Scientific), according to the manufacturer's protocol. RNA was reverse-transcribed using the High-Capacity cDNA Reverse Transcription kit (Thermo Fisher Scientific). Real-time PCR was performed on a Bio-Rad CFX96 machine using SYBR Green mix (Bio-Rad). The relative levels of different transcripts were calculated using the ΔΔCt method and results were normalized based on the expression of GAPDH.

In vitro culture of murine monocytes and flow cytometry

Crude BM cells isolated from C57 BL/6 mice were cultured in RPMI 1640 medium supplemented with 10% FBS, 2 mM L-glutamine, 1% penicillin/streptomycin, and with M-CSF (10 ng ml^{-1}) in the presence of different doses of LPS (from 100 pg ml^{-1} to 1 μg ml^{-1}). TUDCA (500 μM) was also added to the cell cultures in some experiments. Fresh LPS and TUDCA was added to the cell cultures every 2 days. After 5 days, cells were harvested and stained with anti-Ly6C, anti-CD11b and anti-CCR5 antibodies (BioLegend, San Diego, CA). The samples were then analyzed by FACSCanto II (BD Biosciences, San Jose, CA). The data were processed by FACSDiva (BD Biosciences), or Flow Jo (Tree Star, Ashland, OR).

Confocal Microscopy

Cells were fixed with 4% paraformaldehyde, permeabilized with methanol and stained with Cy3-conjugated anti-mouse LAMP1 antibody (Abcam, UK) together with Alexa Fluor 488-conjugated anti-mouse LCIII antibody (Novus Biologicals, Littleton, CO). The samples were analyzed under the Zeiss LSM 510 confocal microscope.

In vitro culture of human monocytes and flow cytometry analyses

Peripheral blood from healthy individuals was purchased from Research Blood Components, LLC (Boston, MA). PBMCs were isolated using Histopaque®-1119 and Histopaque®-1077 (Sigma-Aldrich, St. Louis, MO), and then cultured with RPMI 1640 medium supplemented with 10% fetal bovine serum (FBS), 2 mM L-glutamine, 1% penicillin/streptomycin, together with M-CSF (100 ng ml^{-1}) in the presence of different doses of LPS (5 pg ml^{-1}, 50 pg ml^{-1} and 10 ng ml^{-1}). After 2 days, cells were harvested and stained with anti-CD14,

anti-CD16 and anti-CCR5 antibodies (BioLegend). The samples were then analyzed by FACSCanto II (BD Biosciences). The data were processed by FACSDiva (BD Biosciences), or Flow Jo (Tree Star).

Chemotaxis Assays

Chemotaxis of monocytes in response to CCL3 (100 ng ml^{-1}) and CCL5 (100 ng ml^{-1}) was performed using a 48-well Micro Chemotaxis Chamber (NeuroProbe, Gaithersburg, MD) in which a 8-μm pore size polycarbonate filter separated the upper and the lower chamber. The cells were incubated in RPMI 1640 medium supplemented with 1% BSA, 2 mM L-glutamine, 1% penicillin/streptomycin, 30mM HEPES, and allowed to migrate towards CCL3 or CCL5 for 2 hours. After the migration period, the filters were fixed and stained with Giemsa, and the cells migrated across the filters were counted by light microscopy. The results were expressed as the means ± S.E. of the chemotaxis index (CI), representing the increase in the number of migrated cells in response to chemoattractants compared with spontaneous cell migration (to control medium).

Statistical analysis

Statistical analyses were performed using Prism Version 5 software (GraphPad). Significance of difference was analyzed with a Student *t* test. When more than two groups were compared, one-way ANOVA was performed. Data were presented as means ± SEM. P values less than 0.05 were considered significant.

Results

Impaired cutaneous wound healing in mice pre-conditioned with subclinical super-low dose LPS

Although past evidence suggests a connection between subclinical super-low dose endotoxemia and chronic disease, no data is available to confirm causation. We used the cutaneous wound healing model to test whether injection of super-low dose endotoxin affects the proper course of wound repair. Mice were pre-conditioned *i.p.* with either PBS or super-low dose LPS (5 ng/kg body weight) as shown in Fig. 1A. They were then subjected to a procedure that yields full-thickness cutaneous wounds, and closely observed for recovery. As shown in Fig. 1B, 1C and supplementary Figure S1, the wound closure was significantly impaired in LPS pre-conditioned mice, especially at the later stage of wound healing (10–11 days post wounding; Fig 1C).

In addition to the superficial evaluation of the overall wound size, we evaluated the quality of tissue repair through histological examination. Specifically, we studied the course of blood vessel sprouting and regression in the wound bed, as well as collagen deposition. As shown in Fig. 1D–E, blood vessel sprouting occurs well in the wound tissues of PBS- and LPS-pre-conditioned mice 6 days after wounding. However, the pruning and regression of blood vessels at the late stage of wound repair (d 11) were significantly compromised in LPS-pre-conditioned mice. Collagen deposition was also significantly reduced in the wound beds of LPS-pre-conditioned mice (Fig. 1F–G). An analysis of disease score based on

inflammatory cell infiltration also corroborated with the reduced wound repair in LPS pre-conditioned mice, as shown in Supplementary Figure S2.

Sustained presence of pro-inflammatory monocytes in wound tissues of mice conditioned with super-low dose LPS

Sustained polarization of pro-inflammatory monocytes plays a key role in delayed wound repair [6,27]. Of particular relevance, sustained presence of inflammatory monocytes was shown to negatively affect the resolution of tissue repair through prolonged blood vessel sprouting and impaired pruning [5,28]. However, the agents and mechanisms responsible for the sustained polarization of low-grade inflammatory monocytes were not well understood. Thus, we tested whether super-low dose LPS can induce sustained polarization of low-grade inflammatory monocytes *in vivo*. As measured by immuno-histochemistry, tissue levels of monocytes/macrophages initially rose at day 1 after wounding, and subsequently subsided at day 11 in PBS-pre-conditioned mice (Fig. 2A). In contrast, the tissue levels of monocytes/macrophages remained at a significantly higher level at day 11 in LPS-pre-conditioned mice. Furthermore, flow cytometry of elutriated suspension cells from the wound tissues demonstrated significantly more $CD11b^{+}Ly6C^{high}$ pro-inflammatory monocytes in mice pre-conditioned with LPS as compared to PBS-treated mice, both at day 1 and day 11 after wounding (Fig. 2B). Circulating levels of the $CD11b^{+}Ly6C^{high}$ pro-inflammatory monocytes were also higher in LPS-treated mice than PBS-treated mice (Fig. 2C). Plasma levels of selected cytokines were also raised in LPS-treated mice (Supplementary Figure S3). As a consequence, tissue levels of neutrophils as well as myeloperoxidase (MPO) activities were similarly elevated in mice treated with super-low dose LPS, compared to PBS (Supplementary Figure S4–6).

Polarization of low-grade inflammatory monocytes *in vitro* by sustained challenges with super-low dose LPS

Given our *in vivo* observation of elevated inflammatory monocytes in mice injected with super-low dose LPS, we next examined whether super-low dose LPS may directly modulate the expansion of $CD11b^{+}Ly6C^{high}$ inflammatory monocytes *in vitro*. To this end, we cultured bone marrow-derived monocytes with M-CSF together with varying dosages of LPS for 5 days. As shown in Fig. 3A, continuous incubation with super-low dose LPS significantly expanded the population of the $CD11b^{+}Ly6C^{high}$ inflammatory monocytes *in vitro*. The expansion of the $CD11b^{+}Ly6C^{high}$ inflammatory monocytes reached a plateau upon challenge with the intermediate levels of LPS, and declined with higher dosages (Fig. 3B). We further examined the expression levels of a key chemokine receptor CCR5, representative of inflammatory monocytes in both murine and human systems [3]. Both the percentages of $CCR5^{+}$ monocytes and the mean fluorescent intensities of CCR5 were elevated in cells incubated with super-low dose LPS, but reduced in cells cultured with higher dosages of LPS (Fig. 3B). We further performed real-time RT-PCR analyses of representative inflammatory mediators, and observed that monocytes continually incubated with super-low dose LPS exhibit a unique expression profile distinct from the traditionally defined M1 or M2 subtypes (Supplementary Figure S7). We therefore use the term “low-grade inflammatory monocytes” (M_L) to define this phenotype.

Recent studies indicate that the intermediate $CD14^+CD16^+$ monocytes are the preferential inflammatory subsets in humans [2,3]. This particular subset also expresses high levels of CCR5. Thus, we tested whether LPS may preferentially expand the intermediate inflammatory monocytes in human blood. Since human monocytes are much more sensitive to LPS and probably respond to much lower dosages of LPS, we used a much lower concentration range for the human study. As shown in Fig. 3C, super-low dose LPS selectively and significantly expanded the population of intermediate $CD14^+CD16^+$ $CCR5^+$ monocytes, while higher dosages of LPS drastically reduced this population *in vitro*.

Increased migratory ability of monocytes programmed by super-low dose LPS *in vitro*

Based on our above observation that super-low dose LPS elevates the tissue levels of inflammatory monocytes, we further studied the migratory behavior of monocytes programmed by super-low dose LPS *in vitro*, using a chemotaxis assay in transwell chambers with selective CCR5 agonist CCL3. As shown in Fig. 4A, murine monocytes cultured with super-low dose LPS were more able to migrate toward CCL3. We further demonstrated by real-time RT-PCR a significant induction of *Ccr5* mRNA levels in cells programmed by sustained challenges with super-low dose LPS (Fig. 4B).

Super-low dose LPS polarizes monocytes via cellular stress and IRF5 accumulation

We previously reported that super-low dose LPS selectively induces cellular stress and stress-related kinases such as the c-Jun N-terminal kinase (JNK) in macrophages [29]. Next, we studied whether prolonged challenges of monocytes with super-low dose LPS may sustain JNK activation, and whether the alleviation of cellular stress through the application of TUDCA may reduce the migratory behavior of the inflammatory monocytes. TUDCA has a traditional medicinal role in the treatment of tissue injury [30]. On a molecular level, TUDCA has been shown to be a potent inhibitor of cellular stress and JNK activation [31]. As shown in Fig. 4C, prolonged incubation of monocytes with super-low dose LPS for 5 days led to the activation of JNK, and addition of TUDCA ablated the JNK activation mediated by LPS.

TUDCA may exert its inhibitory effect on JNK through restoring cellular homeostasis [31]. We previously reported that super-low dose LPS disrupts cellular homeostasis by disrupting the orderly fusion of lysosomes with autophagosomes [22]. We therefore tested whether TUDCA may restore the completion of autophagy through facilitating the fusion of autophagosome with lysosome. Indeed, monocytes with prolonged super-low dose LPS challenges experienced a disruption of lysosome-autophagosome fusion, as judged from the separation of LCIII staining and LAMP1 staining observed under confocal microscopy, while application of TUDCA restored this process and the co-localization of LCIII and LAMP1 (Fig. 4D).

IRF-5 was shown to be a signature transcription factor within inflammatory monocytes [32]. We observed that IRF-5 levels were elevated in monocytes programmed by super-low dose LPS, and dramatically reduced in monocytes programmed by higher dose LPS (Fig. 5A). Our data further supports the notion that super-low dose LPS programs monocytes into an $IRF\text{-}5^+$ low-grade inflammatory state. Since IRF-5 protein is known to be modulated by

degradation [33], and lysosome function is among the key mechanisms modulating protein degradation [34], we investigated whether super-low dose LPS may enhance IRF-5 stability through disrupting lysosome function. Western blotting indicated that treatment with the lysosome inhibitor chloroquine increased IRF-5 protein levels in cultured monocytes, suggesting that disruption of lysosome function may account for the enhanced IRF-5 protein stability (Fig. 5A). On the other hand, we TUDCA treatment blocked the induction of IRF-5 by super-low dose LPS (Fig. 5A). To further test the modulation of IRF-5 within the $Ly6C^{high}$ monocyte population, we performed flow cytometry analyses with cultured monocytes. We observed that sustained super-low dose LPS challenges significantly increased the IRF-5 levels within the $Ly6C^{high}$ monocytes (Fig. 5B, C). Application of chloroquine alone raised the IRF-5 levels within the $Ly6C^{high}$ monocytes, mimicking the effect of super-low dose LPS (Fig. 6b). In contrast, application of TUDCA reduced the levels of IRF-5 within the $Ly6c^{high}$ monocytes challenged with super-low dose LPS (Fig. 5B, C).

As shown in Fig. 5D, the application of TUDCA reduced the CCR5 expression induced by super-low dose LPS, and also drastically inhibited the migration of LPS-incubated monocytes toward CCL3 and CCL5 (Fig. 5E).

TUDCA facilitates wound healing *in vivo*

We next tested whether TUDCA may facilitate wound repair in mice pre-conditioned with super-low dose LPS. Indeed, *i.p.* injection of TUDCA dramatically improved the course of wound repair (Fig. 6A–B) and facilitated the pruning and regression of blood vessels at the later stage of wound healing (Fig. 6C–D).

Flow cytometry of inflammatory monocytes *in vivo* showed that mice treated with TUDCA together with super-low dose LPS had lower levels of inflammatory $CD11b^{+}Ly6C^{high}$ monocytes than mice challenged with super-low dose LPS (Fig. 6E). The numbers of infiltrating inflammatory granulocytes within the wound tissues were also reduced in TUDCA-treated mice (Supplementary Figure S8).

Discussion

Our data demonstrates that sustained challenges with super-low dose endotoxin can polarize the low-grade inflammatory monocytes both *in vitro* and *in vivo*. Inflammatory polarization of monocytes as reflected in the sustained expansion and recruitment of inflammatory monocytes could be critically involved in the altered wound healing dynamics. Mechanistically, a disruption of lysosome function in monocytes may contribute to the accumulation of IRF5, a key transcription factor representative of inflammatory monocytes. Our intervention study with TUDCA may hold potential promise in re-balancing monocyte homeostasis that is necessary for effective wound healing.

Our data complement and extend the emerging concept of innate immunity programming [8]. Innate immune cells may be differentially programmed by simultaneous or sequential challenges of distinct innate agonists, as measured by the expression levels of selected cytokines [35]. For example, as compared to naïve monocytes, monocytes previously

"trained" with beta-glucan may express much higher levels of IL-6 when subsequently challenged with LPS [36]. In terms of innate programming by LPS, we and others reported that monocytes/macrophages with an initial challenge of varying dosages of LPS may adopt either a "primed" or "tolerant" state, with regard to the expression of selected pro-inflammatory cytokines [20,21,26,37]. In contrast to these existing reports, this current study is the first to examine the programming of monocytes under continuous and prolonged incubation with LPS. This may better reflect *in vivo* pathophysiological situations in humans with subclinical endotoxemia due to mucosal leakage. Our data reveal that monocytes under prolonged incubation with higher dose LPS exhibit reduced expression of selected inflammatory mediators such as CCR5, reminiscent of the endotoxin-tolerant phenotype. In contrast, monocytes under prolonged and continued incubation with super-low dose LPS exhibit sustained expression of inflammatory cytokines, elevated surface levels of Ly6C as well as chemokine receptor CCR5.

Our data with primary human cells cultured with LPS further confirm this phenomenon. Super-low dose LPS selectively expands the inflammatory intermediate monocyte population, while higher dose LPS dramatically reduced the population of the inflammatory intermediate monocytes. In clinical settings, the intermediate human monocytes have been closely correlated with chronic inflammatory diseases [3,38]. Our data provides a system for future mechanistic studies with regard to the ontology and maintenance of human intermediate inflammatory monocytes.

In the context of wound healing, although a causal connection between the sustained presence of pro-inflammatory monocytes and compromised wound repair is well established [5,7,27,28], the cause and mechanism responsible for the establishment and dynamic "memory" of low-grade inflammatory monocytes were not known. Our current study fills this gap, and reveals that super-low dose LPS can selectively program and sustain inflammatory monocytes both *in vitro* and *in vivo*, and delay effective wound repair. With further pathological relevance, the super-low doses of LPS we used closely resemble plasma circulating levels of LPS in humans with chronic health conditions such as diabetes, aging and chronic inflammation [9,10,39–41]. Extending this correlation, our data suggest causal relevance of super-low dose LPS in selectively programming the low-grade inflammatory monocyte both *in vitro* and *in vivo*.

Although extensive studies exist regarding the effects of higher dose LPS on cellular signaling, very few have examined the effects of pathologically-relevant super-low dose LPS [8]. Mechanistically, our recent reports reveal that super-low dose LPS preferentially utilizes cell surface TLR4 receptor, (rather than endocytosed TLR4), and activates IRAK-1-mediated signaling and JNK activation [20,22,29,42]. Extending these observations, the current work focuses on the modulation of IRF-5, a key polarizing transcription factor involved in the activation of inflammatory monocytes/macrophages [32,43]. The cause and mechanism for the accumulation of IRF-5 in monocyte polarization have not been clarified. Our study provides the first evidence that super-low dose LPS potently programs low-grade inflammatory monocytes by inducing IRF-5. This extends our previous findings and reveals that disruption of lysosome fusion is causally responsible [22]. Furthermore, our data clarify

the role of therapeutic agent TUDCA in facilitating would repair, through restoring lysosome fusion and relieving persistent low-grade JNK activation.

Taken together, the current study reveals the intriguing dynamics of monocyte polarization, and its pathological consequence in wound repair, intervention in which may hold promise for treating chronic wounds and other inflammatory diseases.

Supplementary Material

Refer to Web version on PubMed Central for supplementary material.

Acknowledgments

We thank the members of the Li Lab for constructive discussion and assistance. Funding: This work was supported by the National Institute of Health grants R01 HL115835, R56AI108264 to L.L., and R01AI115986 to H.C. and L.L.

References

1. Auffray C, Sieweke MH, Geissmann F. Blood monocytes: development, heterogeneity, and relationship with dendritic cells. Annual review of immunology. 2009; 27:669–692.
2. Zimmermann HW, Trautwein C, Tacke F. Functional role of monocytes and macrophages for the inflammatory response in acute liver injury. Frontiers in physiology. 2012; 3:56. [PubMed: 23091461]
3. Shimada K. Diversity and plasticity of monocyte subsets. Tipping the delicate balance involved in the pathogenesis of atherosclerosis. Circulation journal : official journal of the Japanese Circulation Society. 2012; 76:2331–2332. [PubMed: 22971906]
4. Ozaki Y, Imanishi T, Taruya A, et al. Circulating CD14+CD16+ monocyte subsets as biomarkers of the severity of coronary artery disease in patients with stable angina pectoris. Circulation journal : official journal of the Japanese Circulation Society. 2012; 76:2412–2418. [PubMed: 22785372]
5. Willenborg S, Lucas T, van Loo G, et al. CCR2 recruits an inflammatory macrophage subpopulation critical for angiogenesis in tissue repair. Blood. 2012; 120:613–625. [PubMed: 22577176]
6. Dal-Secco D, Wang J, Zeng Z, et al. A dynamic spectrum of monocytes arising from the in situ reprogramming of CCR2+ monocytes at a site of sterile injury. The Journal of experimental medicine. 2015
7. Mirza R, Koh TJ. Dysregulation of monocyte/macrophage phenotype in wounds of diabetic mice. Cytokine. 2011; 56:256–264. [PubMed: 21803601]
8. Morris MGE, Li L. Innate immune programming by endotoxin and its pathological consequences. Frontiers in Immunology. 2015; 5:680, 1–8. [PubMed: 25610440]
9. Nymark M, Pietilainen KH, Kaartinen K, et al. Bacterial Endotoxin Activity in Human Serum Is Associated With Dyslipidemia, Insulin Resistance, Obesity, and Chronic Inflammation. Diabetes Care. 2011
10. Frazier TH, DiBaise JK, McClain CJ. Gut microbiota, intestinal permeability, obesity-induced inflammation, and liver injury. JPEN J Parenter Enteral Nutr. 2011; 35:14S–20S. [PubMed: 21807932]
11. Moreno-Navarrete JM, Manco M, Ibanez J, et al. Metabolic endotoxemia and saturated fat contribute to circulating NGAL concentrations in subjects with insulin resistance. Int J Obes (Lond). 2009
12. Wiesner P, Choi SH, Almazan F, et al. Low doses of lipopolysaccharide and minimally oxidized low-density lipoprotein cooperatively activate macrophages via nuclear factor kappab and activator protein-1: possible mechanism for acceleration of atherosclerosis by subclinical endotoxemia. Circulation research. 2010; 107:56–65. [PubMed: 20489162]

13. Qin L, Wu X, Block ML, et al. Systemic LPS causes chronic neuroinflammation and progressive neurodegeneration. Glia. 2007; 55:453–462. [PubMed: 17203472]
14. Manco M, Putignani L, Bottazzo GF. Gut microbiota, lipopolysaccharides, and innate immunity in the pathogenesis of obesity and cardiovascular risk. Endocr Rev. 2010; 31:817–844. [PubMed: 20592272]
15. Sindrilaru A, Peters T, Wieschalka S, et al. An unrestrained proinflammatory M1 macrophage population induced by iron impairs wound healing in humans and mice. The Journal of clinical investigation. 2011; 121:985–997. [PubMed: 21317534]
16. Ishikawa J, Tamura Y, Hoshide S, et al. Low-grade inflammation is a risk factor for clinical stroke events in addition to silent cerebral infarcts in Japanese older hypertensives: the Jichi Medical School ABPM Study, wave 1. Stroke. 2007; 38:911–917. [PubMed: 17272770]
17. West MA, Heagy W. Endotoxin tolerance: A review. Crit Care Med. 2002; 30:S64–S73.
18. Li L, Cousart S, Hu J, et al. Characterization of interleukin-1 receptor-associated kinase in normal and endotoxin-tolerant cells. J Biol Chem. 2000; 275:23340–23345. [PubMed: 10811644]
19. Henricson BE, Manthey CL, Perera PY, et al. Dissociation of lipopolysaccharide (LPS)-inducible gene expression in murine macrophages pretreated with smooth LPS versus monophosphoryl lipid A. Infection and immunity. 1993; 61:2325–2333. [PubMed: 8388859]
20. Deng H, Maitra U, Morris M, et al. Molecular mechanism responsible for the priming of macrophage activation. J Biol Chem. 2013; 288:3897–3906. [PubMed: 23264622]
21. Fu Y, Glaros T, Zhu M, et al. Network topologies and dynamics leading to endotoxin tolerance and priming in innate immune cells. PLoS computational biology. 2012; 8:e1002526. [PubMed: 22615556]
22. Baker B, Geng S, Chen K, et al. Alteration of Lysosome Fusion and Low-grade Inflammation Mediated by Super-low-dose Endotoxin. J Biol Chem. 2015; 290:6670–6678. [PubMed: 25586187]
23. Macedo L, Pinhal-Enfield G, Alshits V, et al. Wound healing is impaired in MyD88-deficient mice: a role for MyD88 in the regulation of wound healing by adenosine A2A receptors. Am J Pathol. 2007; 171:1774–1788. [PubMed: 17974599]
24. Devalaraja RM, Nanney LB, Du J, et al. Delayed wound healing in CXCR2 knockout mice. J Invest Dermatol. 2000; 115:234–244. [PubMed: 10951241]
25. Ishida Y, Gao JL, Murphy PM. Chemokine receptor CX3CR1 mediates skin wound healing by promoting macrophage and fibroblast accumulation and function. J Immunol. 2008; 180:569–579. [PubMed: 18097059]
26. Morris M, Gilliam E, Button J, et al. Dynamic modulation of innate immune response by varying dosages of LPS in human monocytic cells. Journal of Biological Chemistry. 2014; 289:21584–90. [PubMed: 24970893]
27. Van Ginderachter JA. The wound healing chronicles. Blood. 2012; 120:499–500. [PubMed: 22821998]
28. Murray PJ, Wynn TA. Protective and pathogenic functions of macrophage subsets. Nature reviews Immunology. 2011; 11:723–737.
29. Baker B, Maitra U, Geng S, et al. Molecular and cellular mechanisms responsible for cellular stress and low-grade inflammation induced by super-low dose endotoxin. J Biol Chem. 2014; 289:16262–16269. [PubMed: 24759105]
30. Colak A, Kelten B, Sagmanligil A, et al. Tauroursodeoxycholic acid and secondary damage after spinal cord injury in rats. Journal of clinical neuroscience : official journal of the Neurosurgical Society of Australasia. 2008; 15:665–671. [PubMed: 18343118]
31. Engin F, Yermalovich A, Nguyen T, et al. Restoration of the unfolded protein response in pancreatic beta cells protects mice against type 1 diabetes. Science translational medicine. 2013; 5:211ra156.
32. Lawrence T, Natoli G. Transcriptional regulation of macrophage polarization: enabling diversity with identity. Nature reviews Immunology. 2011; 11:750–761.
33. Korczeniewska J, Barnes BJ. The COP9 signalosome interacts with and regulates interferon regulatory factor 5 protein stability. Molecular and cellular biology. 2013; 33:1124–1138. [PubMed: 23275442]

34. Luzio JP, Pryor PR, Bright NA. Lysosomes: fusion and function. Nature reviews Molecular cell biology. 2007; 8:622–632. [PubMed: 17637737]
35. Netea MG, Quintin J, van der Meer JW. Trained immunity: a memory for innate host defense. Cell Host Microbe. 2011; 9:355–361. [PubMed: 21575907]
36. Quintin J, Saeed S, Martens JH, et al. Candida albicans infection affords protection against reinfection via functional reprogramming of monocytes. Cell Host Microbe. 2012; 12:223–232. [PubMed: 22901542]
37. Li L, Jacinto R, Yoza B, et al. Distinct post-receptor alterations generate gene- and signal-selective adaptation and cross-adaptation of TLR4 and TLR2 in human leukocytes. J Endotoxin Res. 2003; 9:39–44. [PubMed: 12691617]
38. Ghattas A, Griffiths HR, Devitt A, et al. Monocytes in coronary artery disease and atherosclerosis: where are we now? Journal of the American College of Cardiology. 2013; 62:1541–1551. [PubMed: 23973684]
39. Erridge C, Attina T, Spickett CM, et al. A high-fat meal induces low-grade endotoxemia: evidence of a novel mechanism of postprandial inflammation. Am J Clin Nutr. 2007; 86:1286–1292. [PubMed: 17991637]
40. Wiedermann CJ, Kiechl S, Dunzendorfer S, et al. Association of endotoxemia with carotid atherosclerosis and cardiovascular disease: prospective results from the Bruneck Study. Journal of the American College of Cardiology. 1999; 34:1975–1981. [PubMed: 10588212]
41. Goto T, Eden S, Nordenstam G, et al. Endotoxin levels in sera of elderly individuals. Clin Diagn Lab Immunol. 1994; 1:684–688. [PubMed: 8556521]
42. Maitra U, Deng H, Glaros T, et al. Molecular mechanisms responsible for the selective and low-grade induction of proinflammatory mediators in murine macrophages by lipopolysaccharide. J Immunol. 2012; 189:1014–1023. [PubMed: 22706082]
43. Lu G, Zhang R, Geng S, et al. Myeloid cell-derived inducible nitric oxide synthase suppresses M1 macrophage polarization. Nature communications. 2015; 6:6676.

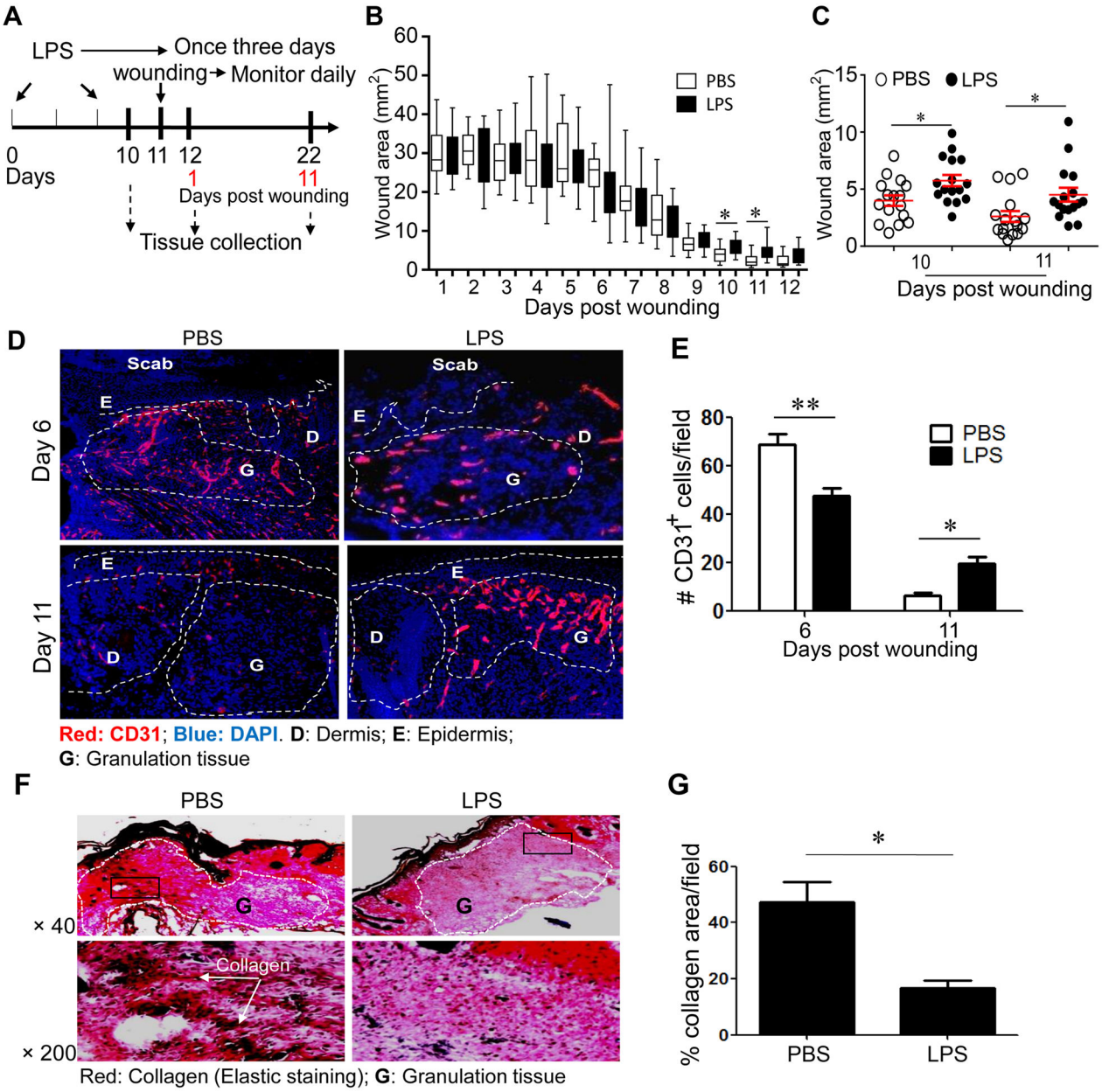

Figure 1. Super-low dose LPS pre-conditioning impairs cutaneous wound healing

(A) LPS treatment regimen and the wounding procedure. **(B, C)** Wounds were monitored and photographed daily. Wound sizes at different time points after wounding are represented in a box and whisker plot. The box regions represent data from the 1st to 3rd quartiles, and the whisker lines represent the remaining outlying data range. Significant differences were apparent on day 10 and 11 after wounding**. (C)** A separate dot plot representing days 10 and 11 is shown with means and standard error bars. Student t test, * $p<0.05$. **(D–E)** Immunohistochemical analyses of CD31-positive endothelial cells as measurements of blood vessel sprouting in wound tissues (**D**). (**E**) The number of CD31-positive cells in the granulation tissues per viewing field at day 6 and 11 after puncture (n=6 fields per slide, 6–7

slide samples per group collected from at least five different animals). *D*: Dermis; *E*: Epidermis; *G*: Granulation tissue; *M*: Muscle; *S*: Scab. Error bars show means ± s.e.m.; * P < 0.05; ** P < 0.01; student t-test. (**F–G)** Super-low dose LPS reduced collagen content in the granulation tissues at day 11 after puncture. (**F**) Elastic staining. Upper panel: × 40, Lower panel: × 200. (**G**) The percentages of collagen in the granulation tissues per viewing field at day 11 after puncture (n = 6 fields per slide, 6–7 slide samples per group from at least five animals). Error bars show means ± s.e.m.; * P < 0.05; ** P < 0.01; student t-test.

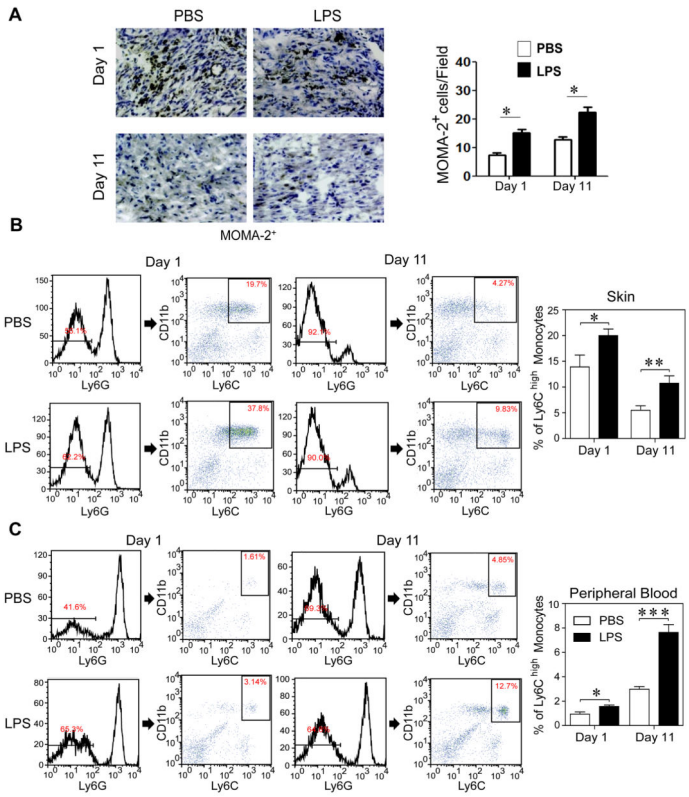

Figure 2. Super-low dose LPS increases recruitment of pro-inflammatory monocytes into wound tissues

(A) Immunohistochemical staining of MOMA-2^+ cells (brown color) around the skin wound at day 1 and day 11 after puncture, with quantification (n = 7). **(B)** Flow cytometry of $Ly6G^-/CD11b^+/Ly6C^{high}$ inflammatory monocytes in wound tissues after puncture. The frequency of inflammatory monocytes among total leukocytes was quantified. Data are shown from PBS- and super-low dose LPS-conditioned mice (day 1, n=6; day 11, n=7). **(C)** Flow cytometry of circulating $Ly6G^-/CD11b^+/Ly6C^{high}$ inflammatory monocytes. Data are shown from PBS- and super-low dose LPS-conditioned mice (day 1, n=6; day 11, n=7). Error bars show means ± s.e.m.; * $P < 0.05$; ** $P < 0.01$; *** $P < 0.001$; student t-test.

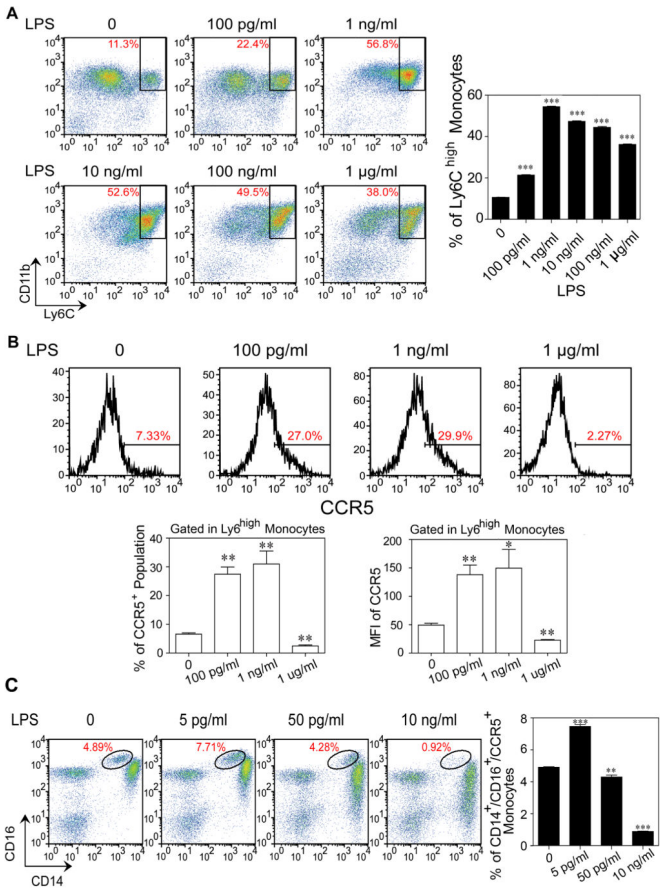

Figure 3. Polarization of inflammatory monocytes by sustained challenges with super-low dose LPS

(A) Expansion of Ly6G^{-}/CD11b^{+}/Ly6C^{high} inflammatory monocytes by super-low dose LPS. BM cells from C57 BL/6 mice were cultured with M-CSF (10 ng ml^{-1}) in the presence of different doses of LPS for 5 days, and fresh LPS was added to the cell cultures every 2 days. Representative flow cytometry plots of the frequencies of Ly6G^{-}/CD11b^{+}/Ly6C^{high} inflammatory monocytes are shown (n=3). **(B)** Induction of CCR5 by super-low dose LPS. The expression levels of CCR5 within Ly6G^{-}/CD11b^{+}/Ly6C^{high} inflammatory monocytes were analyzed by flow cytometry. The frequencies of CCR5^{+} population and the MFI of CCR5 within Ly6C^{high} inflammatory monocytes were quantified (n=3). **(C)** Super-low dose LPS sustains CCR5 expression in human intermediate inflammatory monocytes. Peripheral blood mononuclear cells (PBMCs) isolated from healthy individuals were cultured with M-CSF (100 ng ml^{-1}) in the presence of different doses of LPS for 2 days. Three monocyte sub-populations were detected by flow cytometry based on differential expressions of CD14 and CD16. Frequency of CD14^{+}/CD16^{+} intermediate inflammatory monocytes is displayed. Frequency of CCR5^{+} intermediate inflammatory monocytes was quantified (n=3). Error bars show means ± s.e.m.; * P < 0.05; ** P < 0.01; *** P < 0.001 as compared to controls; one-way ANOVA. Data are representative of three experiments.

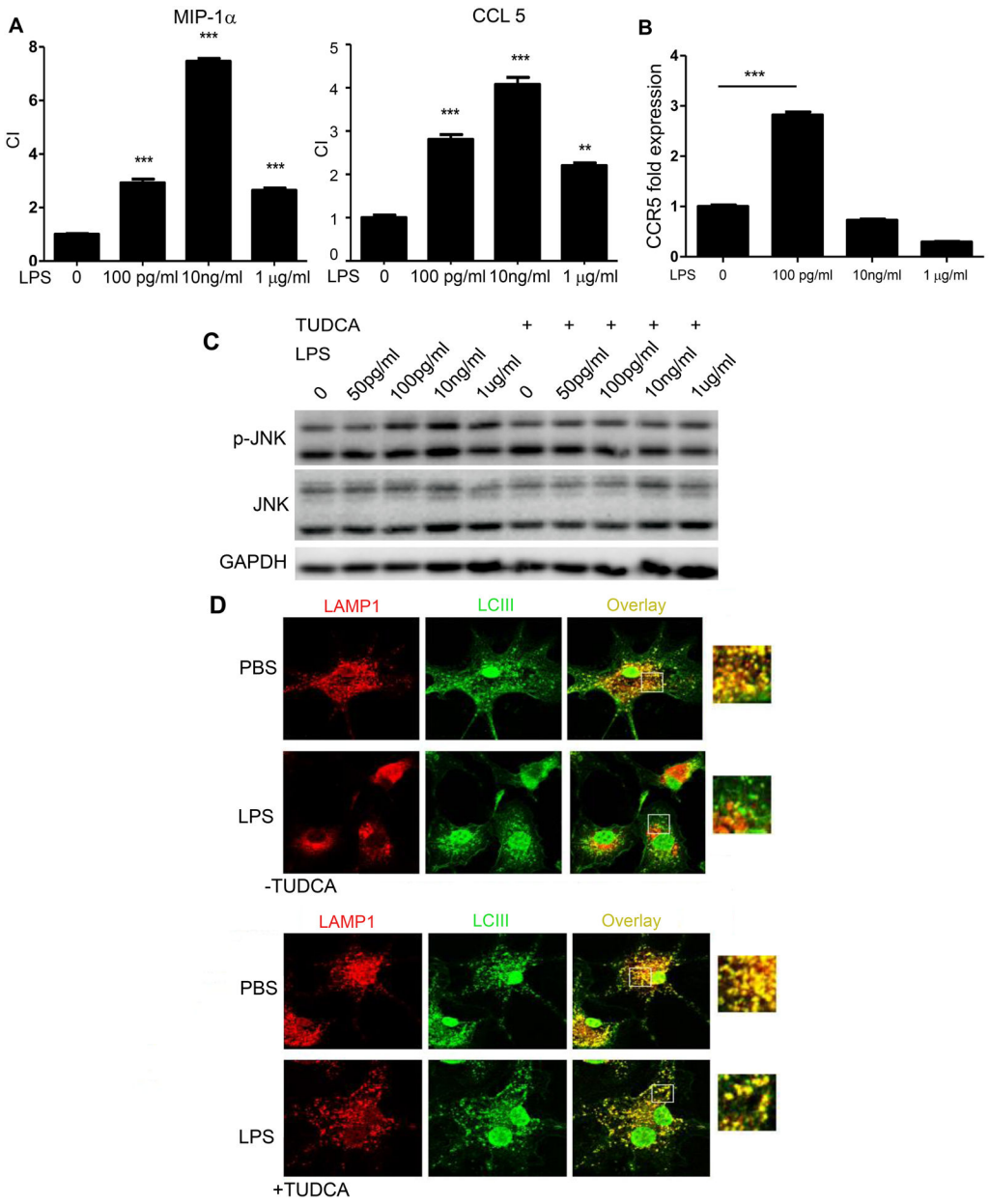

Figure 4. Super-low dose LPS increases migratory ability of monocytes, and polarizes monocytes via sustained cellular stress

(A) *In vitro* chemotaxis assays of monocytes toward CCL3 and CCL5 following continuous incubation with various concentrations of LPS. The chemotaxis index (CI) were quantified (n=3). **(B)** Real-time RT-PCR analyses of chemokine receptor CCR5 (n=3). ***p<0.001, as compared to controls. Error bars show means ± s.e.m.; ** P < 0.01; *** P < 0.001 as compared to controls; one-way ANOVA. Data are representative of three experiments. **(C)** Western blot analysis of phosphorylated JNK in cells treated with LPS or LPS plus TUDCA. Total JNK levels served as controls. **(D)** Restoration of autophagy completion by TUDCA. Cultured monocytes were seeded on coverslips and treated with or without super-low dose LPS (100 pg ml^{-1}) for 24 h. TUDCA (500 μM) was added to some cultures. Cells were then

stained with anti-LAMP1 and anti-LCIII antibodies after starvation. The fusion of lysosomes with autophagosomes was visualized by confocal microscopy. Data represent three experiments.

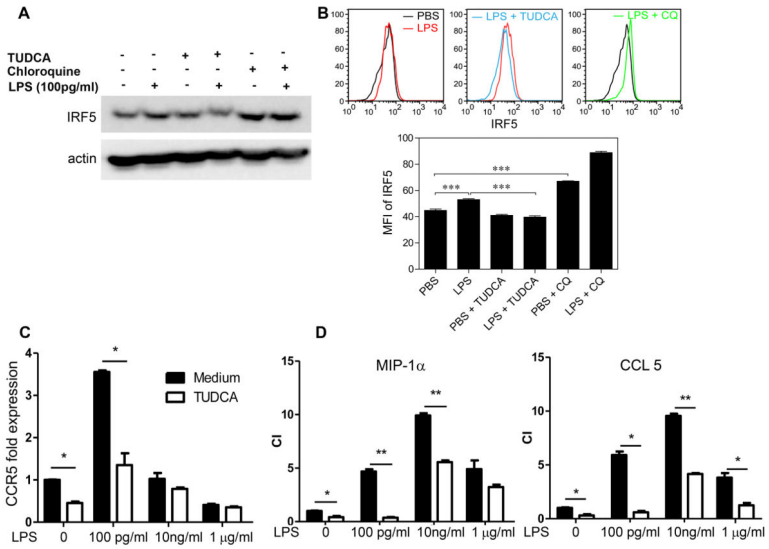

Figure 5. Super-low dose LPS polarizes monocytes via IRF5 accumulation

Monocytes from C57BL/6 mice were cultured with M-CSF (10 ng/ml) in the presence super low dose LPS (100 pg ml^{-1}) for 5 days, and TUDCA (10 nM) or chloroquine (CQ, 1 μM) was also added to some cultures. Fresh LPS, TUDCA and CQ were added to the cell cultures every 2 days. **(A)** Expression levels of IRF5 in monocytes analyzed by Western blot. **(B)** Expression levels of IRF5 within $CD11b^{+}/Ly6C^{high}$ inflammatory monocytes analyzed by flow cytometry. The MFI of IRF5 within $CD11b^{+}/Ly6C^{high}$ inflammatory monocytes was quantified (n = 3). **(C)** Real-time RT-PCR analyses of *Ccr5* levels in monocytes treated with either LPS alone or LPS plus TUDCA (n=3). **(D)** Chemotaxis assays of cultured monocytes toward CCR5 ligands, CCL3 and CCL5. The chemotaxis index (CI) were quantified (n=3). Error bars show means ± s.e.m.; * $P < 0.05$; ** $P < 0.01$; *** $P < 0.001$; one-way ANOVA. Data are representative of three experiments.

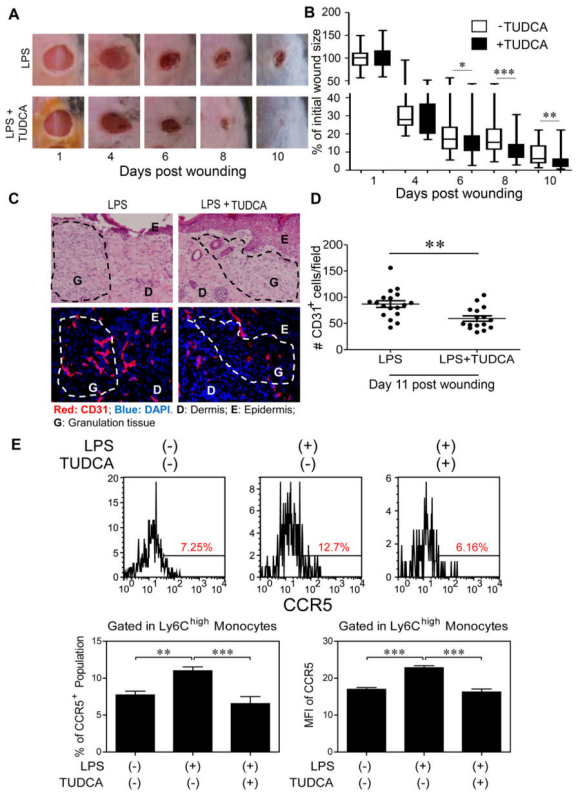

Figure 6. TUDCA facilitates wound healing *in vivo*

Two groups of mice were injected *i.p.* with super-low dose LPS (5 ng/kg body weight) three times for 10 days before skin puncture and once every three days after puncture. After puncture, one group of mice was injected *i.p.* with TUDCA (5 mg/kg) daily for 10 days. **(A)** Wounds were monitored daily. Wound areas (% initial wound size, n>8) over the total observation periods in a box and whisker plot (**B**). Student t test, *, $P < 0.05$; **, $P < 0.01$; ***, $P < 0.001$. **(C)** H&E (**C, top panel**) and immuno-histochemical (**C, bottom panel**) staining of CD31-positive endothelial cells in skin as measurements of blood vessel sprouting within the wound (n=6 fields per slide, 6–7 slides per group). (**D**) Dot plot representing number of CD31-positive cells per viewing field. Error bars represent means ± s.e.m. Student t test, **, $P < 0.01$. **(E)** Peripheral blood cells were collected and CCR5 within $Ly6G^{-}/CD11b^{+}/Ly6C^{high}$ inflammatory monocytes was analyzed by flow cytometry. The frequency of $CCR5^{+}$ population and MFI of CCR5 within $Ly6C^{high}$ inflammatory monocytes were quantified (n>5). Error bars show means ± s.e.m.; ns, not significant; * $P < 0.05$; **, $P < 0.01$; ***, $P < 0.001$; one-way ANOVA.